

SEQUENTIAL DECODING  
ON INTERSYMBOL INTERFERENCE CHANNELS  
WITH APPLICATION TO MAGNETIC RECORDING

A THESIS  
SUBMITTED TO THE DEPARTMENT OF ELECTRICAL  
AND ELECTRONICS ENGINEERING  
AND THE INSTITUTE OF ENGINEERING AND  
SCIENCES OF BILKENT UNIVERSITY  
IN PARTIAL FULFILLMENT OF THE REQUIREMENTS  
FOR THE DEGREE OF  
MASTER OF SCIENCE

By  
Murat ALANYALI  
June 1990

QA  
267.5  
.54  
A43  
1990



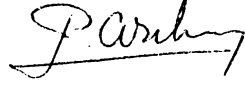
SEQUENTIAL DECODING  
ON INTERSYMBOL INTERFERENCE CHANNELS  
WITH APPLICATION TO MAGNETIC RECORDING

A THESIS  
SUBMITTED TO THE DEPARTMENT OF ELECTRICAL AND ELECTRONICS  
ENGINEERING  
AND THE INSTITUTE OF ENGINEERING AND SCIENCES  
OF BILKENT UNIVERSITY  
IN PARTIAL FULFILLMENT OF THE REQUIREMENTS  
FOR THE DEGREE OF  
MASTER OF SCIENCE

By  
Murat Alanyalı  
June 1990

QA  
267.5  
.S4  
A43  
1990  
S.2298

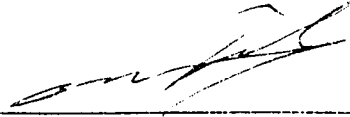
I certify that I have read this thesis and that, in my opinion, it is fully adequate, in scope and in quality, as a thesis for the degree of Master of Science.



---

Associate Prof. Dr. Erdal Arıkan (Principal Advisor)

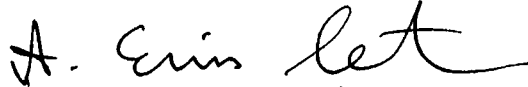
I certify that I have read this thesis and that, in my opinion, it is fully adequate, in scope and in quality, as a thesis for the degree of Master of Science.



---

Associate Prof. Dr. Melek Yücel

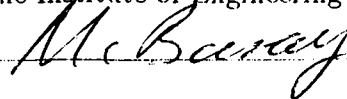
I certify that I have read this thesis and that, in my opinion, it is fully adequate, in scope and in quality, as a thesis for the degree of Master of Science.



---

Assistant Prof. Dr. Enis Çetin

Approved for the Institute of Engineering and Sciences:



---

Prof. Dr. Mehmet Baray  
Director of Institute of Engineering and Sciences

## ABSTRACT

### SEQUENTIAL DECODING ON INTERSYMBOL INTERFERENCE CHANNELS WITH APPLICATION TO MAGNETIC RECORDING

Murat Alanyalı

M.S. in Electrical and Electronics Engineering

Supervisor: Assoc. Prof. Dr. Erdal Arıkan

June, 1990

In this work we treat sequential decoding in the problem of sequence estimation on intersymbol interference ( ISI ) channels. We consider the magnetic recording channel as the particular ISI channel and investigate the coding gains that can be achieved with sequential decoding for different information densities. Since the cutoff rate determines this quantity , we find lower bounds to the cutoff rate.

The symmetric cutoff rate is computed as a theoretical lower bound and practical lower bounds are found through simulations. Since the optimum decoding metric is impractical, a sub-optimum metric has been used in the simulations. The results show that this metric can not achieve the cutoff rate in general, but still its performance is not far from that of the optimum metric.

We compare the results to those of Immink[9] and see that one can achieve positive coding gains at information densities of practical interest where other practical codes used in magnetic recording show coding loss.

Key words: Sequential decoding, intersymbol interference, cutoff rate, decoding metric.

## ÖZET

### MANYETİK KAYITTA UYGULAMASI İLE SEMBOLLER ARASI GİRİŞİM KANALLARDA ARDIŞIK ÇÖZÜMLEME

Murat Alanyalı

Elektrik ve Elektronik Mühendisliği Bölümü Yüksek Lisans

Tez Yöneticisi: Doç. Dr. Erdal Arıkan

Haziran, 1990

Bu çalışmada semboller arası girişim kanallarında (SAG) dizi tahmini probleminde ardışık çözümleme ele alınır. Özel SAG kanal olarak manyetik kayıt kanalı düşünülür ve değişik bilgi yoğunlukları için ardışık çözümleme ile elde edilebilecek kodlama kazançları araştırılır. Bu miktar kesilim hızı tarafından belirlendiği için kesilim hızına alt sınırlar bulunur.

Teorik bir alt sınır olarak simetrik kesilim hızı hesaplanır ve pratik sınırlar simülasyonlarla bulunur. Optimum çözümleme metriği uygulanabilir olmadığı için simülasyonlarda optimuma yakın bir metrik kullanılır. Sonuçlar bu metriğin genelde kesilim hızına ulaşamadığını, ancak performansının optimum metriktan çok uzak olmadığını gösterir.

Sonuçlar İmmink'in [9] sonuçları ile karşılaştırılır ve manyetik kayıta kullanılan pratik kodların kodlama kaybı gösterdiği bilgi yoğunluklarında kodlama kazancı elde edilebileceği görülür.

Anahtar sözcükler: Ardışık çözümleme, semboller arası girişim, kesilim hızı, çözümleme metriği.

## ACKNOWLEDGEMENT

I am indebted to Assoc. Prof. Dr. Erdal Arıkan who made this work possible with his invaluable guidance and suggestions.

# Contents

<b>1</b>	<b>INTRODUCTION</b>	<b>1</b>
1.1	ISI Channel Model . . . . .	2
1.2	The Magnetic Recording Channel . . . . .	4
1.3	Sequential Decoding . . . . .	5
1.4	Cutoff Rate of Channels with ISI . . . . .	6
1.5	The Coding Gain . . . . .	7
<b>2</b>	<b>SEQUENTIAL DECODING ON THE MAGNETIC RECORDING CHANNEL</b>	<b>9</b>
2.1	Coding Techniques for the Magnetic Recording Channel . . . . .	10
2.2	Trellis Coding along with Sequential Decoding	11
2.2.1	The Symmetric Cutoff Rate . . . . .	12
2.2.2	The Decoding Metric . . . . .	13
2.2.3	Simulation Results . . . . .	16
<b>3</b>	<b>CONCLUSION</b>	<b>20</b>
<b>A</b>	<b>COMPUTATION RESULTS OF SEQUENTIAL DECODING</b>	<b>21</b>



# Chapter 1

## INTRODUCTION

Intersymbol interference ( ISI ) arises in pulse modulation systems on time-dispersive channels whenever the transmitted pulse does not completely die away before the transmission of the next. The optimum maximum likelihood receiver structure for finite ISI channels perturbed by additive white gaussian noise ( AWGN ) is due to Forney [1]. This structure consists of a whitened matched filter, a symbol-rate sampler, and the Viterbi algorithm as a recursive nonlinear processor. Although it is the simplest known way of optimal maximum likelihood sequence estimation, the Viterbi algorithm is impractical for channels with large ISI, because its complexity grows exponentially with the length of the channel response. For this reason there is a recent interest in effective decoding methods providing good performance-complexity tradeoff.

Earlier works were centered on decision feedback equalization ( DFE ) methods utilizing a linear processor ( see for example [2] ). DFE reduces noise enhancement of linear feedback but still has the problem of error propagation. Alternative to these structures there is a considerable number of recent works employing reduced state sequence estimation along with decision feedback [3, 4, 5, 6]. These estimators combine the Viterbi algorithm with decision feedback to search a reduced state trellis.

Up to now, sequential decoding algorithms have received scant attention in the problem of detection on ISI channels. In 1966 Chang and Hancock developed a receiver with a sequential algorithm for maximum a posteriori detection, whose structure and complexity grows linearly with the message length [7]. A similar algorithm for symbol by symbol decoding with a fixed structure is due to Abend and Fritchman [8].

In this work we study the Fano sequential decoding algorithm on ISI channels with AWGN. In particular we consider the noisy magnetic recording channel, and compare the performance of trellis coding along with Fano algorithm with a number of coding

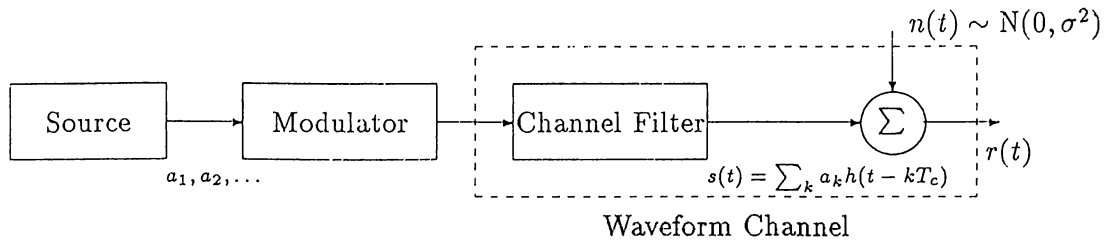


Figure 1.1. The basic intersymbol interference channel with PAM modulation.

schemes according to their asymptotic coding gains. Our main result is that arbitrary positive coding gains can be achieved with the Fano algorithm at information densities of practical interest, where all other coding schemes show a substantial coding loss.

The organization of Chapter 1 is as follows: In Section 1.1 we introduce our treatment of ISI channels. Section 1.2 consists of a description and a simplified model of the magnetic recording channel. In Section 1.3 we make a brief definition of sequential decoding algorithms and comment on their computational problems. Section 1.4 deals with the cutoff rate of ISI channels. Section 1.5 consists of the definition of coding gain.

## 1.1 ISI Channel Model

We consider the Pulse Amplitude Modulation model of Figure 1.1. The source outputs  $a_k$  belong to a finite alphabet  $\mathcal{K}$ , and a new input is introduced to the channel every  $T_c$  seconds.

The waveform  $h(t)$ , which is the convolution of the channel impulse response and the modulation pulse, characterizes the channel. Intersymbol interference occurs among  $L$  consecutive symbols where  $L$  is the smallest integer such that  $h(t) = 0$  for  $t \geq LT_c$ .

On the receiver side, the received signal  $r(t)$  is sampled by a filter matched to  $h(t)$ , and the quantities

$$r_k \triangleq \int_{-\infty}^{+\infty} r(t)h(t - kT_c)dt \quad (1.1)$$

are obtained, forming a set of sufficient statistics for the estimation of the source sequence.

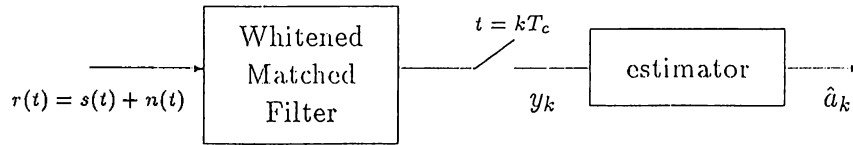


Figure 1.2. The optimum receiver for a channel with intersymbol interference.

Since

$$r(t) = \sum_k a_k h(t - kT_c) + n(t) \quad (1.2)$$

we have

$$r_k = \sum_{i=-L}^L R_i a_{k-i} + \hat{n}_k \quad (1.3)$$

where

$$R_i \triangleq \int_{-\infty}^{+\infty} h(t)h(t - iT_c)dt \quad (1.4)$$

and  $\hat{n}_k$ 's are colored noise terms with

$$E\{\hat{n}_k \hat{n}_j\} = \sigma^2 R_{k-j} \quad (1.5)$$

The sequence  $\{r_k\}$  is passed through a whitening filter which is described in detail in [1], without causing any further degradation in the performance of the receiver and the sequence  $\{y_k\}$

$$y_k = \sum_{j=0}^L f_j a_{k-j} + n_k \quad (1.6)$$

is obtained, where

$$R_i = \sum_{j=i}^L f_j f_{j-i} \quad i = 0, 1, \dots, L \quad (1.7)$$

and  $n_k$ 's are independent Gaussian random variables with variance  $\sigma^2$ . Hence the receiver structure can be pictured as in Figure 1.2.

## 1.2 The Magnetic Recording Channel

Magnetic recording is achieved by moving the recording head with a varying magnetic field past the magnetic medium. The head is a transducer that converts electrical signals to magnetization patterns. The current through the head coil, which is driven by the information source, generates demagnetization patterns in the medium. These fields characterize the source in a unique way through the voltage induced on a coil moving relative to the medium. This process is called the readback procedure. The fact that the magnetic field of the writing head is not space limited and the readback process is linear, gives rise to intersymbol interference.

An important channel parameter is the pulse-width  $PW_{50}$ , which is a measure of the dispersivity of the channel. Very briefly,  $PW_{50}$  is the longitudinal distance between the points that the pulse is applied and the readback voltage drops to 50% of its peak value.

Our analysis of the magnetic recording channel is based on the Lorentzian channel model. According to this model the channel step response  $g(t)$  is approximated by

$$g(t) = \frac{v}{PW_{50}} \cdot \frac{1}{1 + \left(\frac{2vt}{PW_{50}}\right)^2} \quad (1.8)$$

where  $v$  is the medium to head speed.

In our treatment the source alphabet  $\mathcal{K} = \{-1, +1\}$  and the medium is assumed to be recorded as perfect full  $T_c$  sec. pulses.

$$P_{T_c}(t) = \begin{cases} \sqrt{E_b} & -\frac{T_c}{2} < t < \frac{T_c}{2} \\ 0 & \text{else} \end{cases}$$

The channel waveform  $h(t)$  is then given by

$$h(t) = \sqrt{E_b} \left[ g\left(t + \frac{T_c}{2}\right) - g\left(t - \frac{T_c}{2}\right) \right] \quad (1.9)$$

Using definition 1.4 the autocorrelation coefficients  $R_k$  can be found parametrically as [9]

$$R_k = E_c \frac{\alpha^2(\alpha^2 + T_c^2 - 3k^2T_c^2)(T_c^2 + \alpha^2)}{k^6T_c^6 - 2k^4T_c^6 + 3k^4T_c^4\alpha^2 + k^2T_c^6 + 3k^2T_c^2\alpha^4 + T_c^4\alpha^2 + 2T_c^2\alpha^4 + \alpha^6} \quad (1.10)$$

where

$$E_c = E_b \frac{\pi}{2} \frac{T_c^2}{\alpha(T_c^2 + \alpha^2)} \quad (1.11)$$

and  $\alpha = \frac{PW_{50}}{\nu}$ .

### 1.3 Sequential Decoding

A sequential decoder is a tree search algorithm which decodes a code with a tree structure by making tentative hypotheses on successive branches of the code tree. The decoder extends the path which appears the most probable, and when subsequent branches indicate an incorrect hypothesis, it goes back and tries another path. While the Viterbi decoder extends all the paths that can potentially be the best, the sequential decoder works with one path at a time, severely limiting the complexity.

We define the metric <sup>1</sup> of code span  $x^l = (x_0, x_1, \dots, x_l)$  based on the reception of the channel output sequence  $y^l = (y_0, y_1, \dots, y_l)$  as

$$\Gamma(x^l, y^l) = \log_2 \frac{P_l(y^l | x^l)}{w_l(y^l)} - lR \quad (1.12)$$

In this expression  $R$  is the code rate in bits,  $P_l(\cdot | \cdot)$  is the conditional probability distribution function (p.d.f.) of the channel output sequence given the input sequence, and  $w_l(\cdot)$  is the marginal p.d.f. of the channel output sequence.

This metric allows the decoder to identify the most likely path based on the information available at each stage. The essential property of a sequential decoder is that

<sup>1</sup>This is not a metric in the mathematical sense.

its decisions are independent of the future received symbols. Therefore the function of the decoder is to hypothesize in such a way that  $\Gamma(x^l, y^l)$  increases in an average sense.

The particular sequential decoding algorithm that is investigated in this work is the Fano algorithm. One can refer to [10, section 6.9] for a detailed description.

**Computation of the Sequential Decoder :** The number of hypotheses that a sequential decoder makes in decoding a received sequence depends on the code, the transmitted sequence, and the received sequence, hence is a random variable. The behavior of the computation has been studied in detail by Gallager [10] for the memoryless case, and it is shown that the average number of computations per tree node is finite if  $R < R_0$ , where  $R_0$  is the cutoff rate of the channel which will be described in more detail in section 1.4. The same result applies to the case of channels with memory in a similar manner with a modified metric which carries the memory of the channel at each step.

By increasing the constraint length of the code one can achieve arbitrarily small error probabilities without causing significant increase in the computation. Hence the performance of sequential decoders is not limited by the probability of error, however in practice one can not use a sequential decoder at rates above the cutoff rate.

## 1.4 Cutoff Rate of Channels with ISI

A channel with finite intersymbol interference is an indecomposable finite state channel and the cutoff rate,  $R_0$ , is given by the zero rate intercept of Gallager random coding exponent [10, section 5.9]. For unquantized channel outputs  $R_0$  is defined in units of bits/symbol as

$$R_0 = \lim_{N \rightarrow \infty} -\frac{1}{N} \log_2 \left[ \min_{Q(\cdot)} \int \left( \sum_{x^N} Q(x^N) \sqrt{P(y^N | x^N, s_0)} \right)^2 dy^N \right] \quad (1.13)$$

where  $s_0$  is the channel state at time zero <sup>2</sup>,  $N$  is the block length of the channel input and output sequences  $x^N$  and  $y^N$  respectively. The minimization is performed over all input distributions  $Q(\cdot)$ .

The computation of  $R_0$  through the minimization is difficult to perform, so the symmetric cutoff rate  $\tilde{R}_0$  has been defined [11] as a lower bound to  $R_0$ , by evaluating

<sup>2</sup>For an indecomposable channel  $R_0$  is independent of  $s_0$ .



the right hand side of equation 1.13 at the uniform input distribution.

For ISI channels with AWGN, the symmetric cutoff rate for binary inputs,  $\tilde{R}_0^b$ , is given by [12]

$$\tilde{R}_0^b = \lim_{N \rightarrow \infty} -\frac{1}{N} \log_2 \left[ \frac{1}{2^{2N}} \sum_{m=0}^{2^N-1} \sum_{n=0}^{2^N-1} \exp\{-\eta \|d_{mn}^N\|^2/4\} \right] \quad (1.14)$$

In this expression  $\eta$  is the signal to noise ratio and  $d_{mn}^N$  is the normalized Euclidean distance vector between two noiseless channel output sequences.

The symmetric cutoff rate for ISI channels with AWGN can be computed by making use of eigenvalue techniques [12]. For a channel with ISI length  $L$ , computation of  $\tilde{R}_0^b$  necessitates finding the largest eigenvalue of a  $(\frac{3^L+1}{2}) \times (\frac{3^L+1}{2})$  matrix, hence it is still impractical to compute the symmetric cutoff rate for moderate values of  $L$ . In this thesis work, we have computed  $\tilde{R}_0^b$  for  $L$  in the range of 6 to 10. Typical computation times are given Table 2.2.

## 1.5 The Coding Gain

The usual figure of merit of communication systems is the signal to noise ratio that is required to achieve a certain probability of error. Coding gain describes the amount of improvement in this quantity when a particular coding scheme is used. The asymptotic coding gain, in which we are interested in the course of this work, is the value of the coding gain for asymptotically low noise power.

For the AWGN channel with ISI, the probability of error is lower bounded and for large signal to noise ratio well approximated by

$$\Pr[\text{error}] \gtrsim N_{\min} Q\left(\frac{d_{\min}}{2\sigma}\right) \quad (1.15)$$

where  $\sigma^2$  is the noise variance,  $d_{\min}$  is the minimum Euclidean distance between any two distinct channel filter output sequences,  $N_{\min}$  is the average number of nearest neighbor sequences [13].

Since

$$Q(x) \lesssim \exp\left\{-\frac{x^2}{2}\right\} \quad (1.16)$$

for small  $\sigma^2$ , the coded and uncoded schemes will have the same error probability if

$$N_{\min}^{\text{coded}} \exp\left\{-\frac{\left(\frac{d_{\min}^{\text{coded}}}{2\sigma}\right)^2}{2}\right\} = N_{\min}^{\text{uncoded}} \exp\left\{-\frac{\left(\frac{d_{\min}^{\text{uncoded}}}{2\sigma}\right)^2}{2}\right\}$$

Taking the logarithm of both sides and noting that  $N_{\min}$  terms are negligible for small  $\sigma$ , the asymptotic coding gain  $G$  is given in decibels by

$$G = 20 \log_{10} \left[ \frac{d_{\min}^{\text{coded}}}{d_{\min}^{\text{uncoded}}} \right] \quad (1.17)$$

## Chapter 2

# SEQUENTIAL DECODING ON THE MAGNETIC RECORDING CHANNEL

A major problem in magnetic recording is intersymbol interference as we dealt with in Section 1.2. Other imperfections such as the noise generated by the electronic circuits and noise arising from the magnetic properties of the medium corrupt the readback voltage. These effects are usually modelled as additive white Gaussian noise. Technical problems which can not be handled analytically are neglected in this study, making the results comparable to those of Immink [9].

In Section 2.1 we present the noise immunity of the state of the art codes used in magnetic recording, which is reported by Immink. In Section 2.2 we treat the sequential decoding on the magnetic recording channel based on the cutoff rate. Theoretical lower bounds to the performance of sequential decoding are given in Section 2.2.1. In Section 2.2.2 we deal with the practical problem of decoding metric selection. Section 2.2.3 consists of simulation results and performance evaluation of sequential decoding. The relevant parameters of the channel that are used in this study are given in Table 2.1.

Head gap	0.7 $\mu\text{m}$
Head-tape speed, $v$	65 m/sec
Pulse-width, $PW_{50}$	1.565 $\mu\text{m}$
$E_b$	$2.2 \times 10^{-7}$

Table 2.1. Properties of the storage system.

## 2.1 Coding Techniques for the Magnetic Recording Channel

In the following we introduce briefly three coding techniques used in magnetic recording and define the normalized information density,  $S$ , which is the primary parameter that we use in evaluating the performance of different coding schemes.

One of the most widely used codes in magnetic storage systems is run length limited ( RLL ) codes. There is a considerable amount of literature on this subject. RLL codes are characterized by two parameters (  $d, k$  ) which represent the minimum and maximum runlength of a symbol respectively. In the application of RLL codes in magnetic recording, the minimum runlength constraint,  $d$ , is used to reduce the intersymbol interference, and the maximum runlength constraint,  $k$ , is imposed to ensure frequent information for clock synchronization.

Simple dc-free codes, such as Manchester code, have been used in many of the earlier magnetic storage systems. As the name implies dc-free codes have no average power at zero frequency. Dc-free codes fit well to the technical properties of the storage systems such as ac coupling to the rotary head system.

Wolf and Ungerboeck [14] have recently studied trellis coding techniques along with Viterbi algorithm in partial response ( 1 - D ) channels, and showed that error probabilities close to that of a memoryless channel can be achieved using trellis coding with a precoder. The encoder supports technical considerations such as avoiding infinite runs of identical symbols as well. The partial response channel coincides with the magnetic recording channel at asymptotically low information densities, hence this particular trellis code has been considered for magnetic recording.

The normalized information density,  $S$ , is defined in dimensionless quantities as

$$S = \frac{PW_{50}}{vT} \quad (2.1)$$

where  $\frac{1}{T}$  is the bit rate of the binary information source. The information density that is relevant to practical implementation is reported to be 2.0 [9].

The asymptotic coding gains of the codes mentioned above have been found by finding their free distances using exhaustive computer search. The resulting picture which is due to Immink is given Figure 2.1. The analysis indicates that all the coding

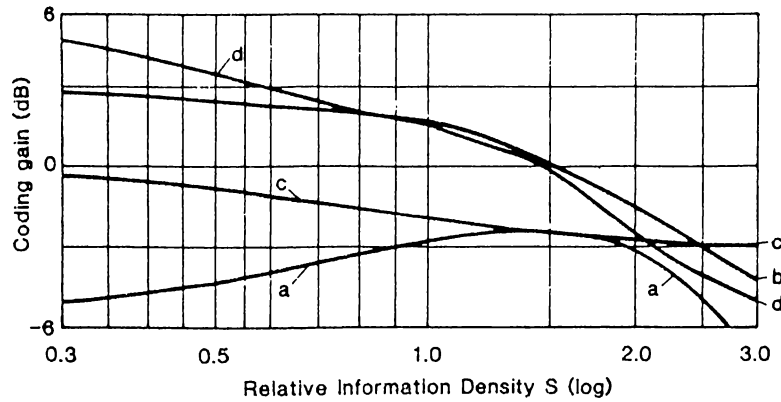


Figure 2.1. Coding gain versus information density  $S$  of (a) partial response class IV detection of uncoded information, (b) dc free code, (c) RLL code, (d) trellis code of constraint length 4.

schemes show a substantial coding loss at information densities of practical interest<sup>1</sup>.

## 2.2 Trellis Coding along with Sequential Decoding

We consider Figure 2.2 as the equivalent discrete time channel model, which is due to Section 1.1. It is assumed that the source generates a binary symbol every  $T$  seconds and the encoder sends a symbol  $x_k \in \{+1, -1\}$  through the channel every  $T_c$  seconds. Hence the code rate is given in bits/symbol by

$$R = \frac{T_c}{T} \quad (2.2)$$

Since we use a sequential decoder, our primary interest is the cutoff rate,  $R_0$ . Note that the channel filter coefficients,  $\{f_k\}$  are determined by  $T_c$ , therefore this parameter determines equivalent discrete channel and the cutoff rate. Contrary to the Viterbi algorithm, the constraint length of the code does not introduce practical limits for sequential decoders, so one can achieve arbitrary positive coding gains by choosing the source bit rate  $T$  so as to satisfy

$$\frac{T_c}{T} < R_0^{T_c} \quad (2.3)$$

<sup>1</sup>Coding loss due to a coding scheme seems confusing. One should note that the codes studied in [9] are weak codes (this is mostly caused by practical limits), and these codes are not designed for high information densities. However, the correctness of the conclusions in [9] is beyond the scope of this work.

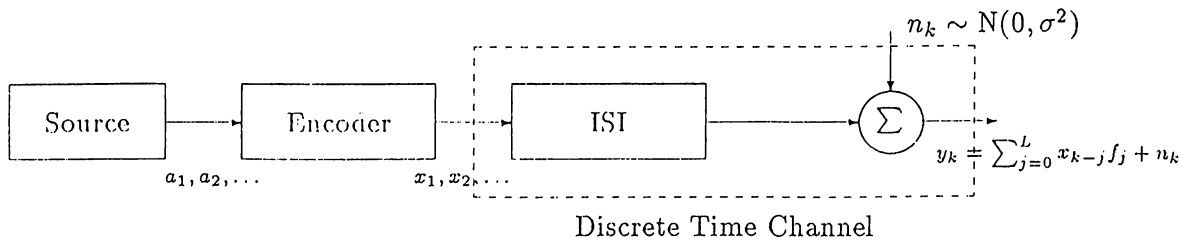


Figure 2.2. Discrete time equivalent of trellis coding on the ISI channel.

We define the cutoff density  $S_0$  for a magnetic recording channel as

$$S_0 \triangleq \frac{PW_{50}}{v} \frac{R_0^{T_c}}{T_c} \quad (2.4)$$

For a fixed value of  $T_c$  one can make use of sequential decoding provided that

$$S < S_0 \quad (2.5)$$

To make our results comparable to those of Immink, we assume a small noise variance of  $\sigma^2 = 0.1$  and look for  $T_c$  values for which the cutoff density exceeds 2.0.

The channel filter coefficients are derived from the autocorrelation coefficients  $\{R_k\}$  which is given in Equation 1.10. In our analysis we truncate the channel coefficients whose magnitudes are less than 5% of that of the coefficient with maximum magnitude. Simulations yield that there is no significant change in the number of computations, hence the cutoff rate, when the truncation rule is lowered to 1%. Further details about the simulations are given in Appendix A.

In the following subsections we provide lower bounds to the cutoff rate through theoretical treatment and simulations. We also deal with the problem of decoding metric selection.

### 2.2.1 The Symmetric Cutoff Rate

The symmetric cutoff rate defined Section 1.4 is asymptotically tight to  $R_0$ , so is a good estimate in the case of small noise power. An efficient algorithm for the computation of the symmetric cutoff rate has recently been proposed by Hirt [12]. However the



$T_c(\eta\text{sec})$	$L$	$\tilde{R}_0^b$	time(sec)
7.85	10	0.9930	919099
8.50	9	0.9985	30912
9.15	9	0.9997	49887
9.80	8	0.9999	4087
10.45	8	0.9999	4395
11.10	7	0.9999	795
11.75	7	0.9999	723
12.40	6	1.0000	78
13.05	6	1.0000	86
13.70	6	1.0000	96
14.35	6	1.0000	74

Table 2.2. Symmetric cutoff rates of the magnetic recording channel.

complexity of the algorithm is exponential in the length of the channel filter,  $L$ . In Table 2.2 we list the  $\tilde{R}_0^b$  values, whose computations were possible in practical sense.

### 2.2.2 The Decoding Metric

The decoding metric of Equation 1.12 in Section 1.3 induces a practical problem in sequential decoding for channels with memory. The reason is that the metric carries all the information about the channel outputs at each stage, and in general the term  $w(y_n | y_{n-1}, y_{n-2}, \dots, y_0)$  is not easy to represent in a compact form.

Arikan [15] has shown that the optimum metric is not unique for memoryless channels. Following his approach, one can define

$$\hat{\Gamma}(x^l, y^l) = \log_2 \frac{\sqrt{P(y^l | x^l)}}{\sum_{\tilde{x}^l} Q(\tilde{x}^l) \sqrt{P(y^l | \tilde{x}^l)}} - lR \quad (2.6)$$

as an alternate optimum decoding metric for channels with memory. However this metric has the additional practical problem that its computation grows with the depth of the tree since it can not be computed in an additive manner.

In the view of the foregoing, we look for sub-optimum but practical ways of sequential decoding. As an alternative we treat the output sequence  $\{y_n\}$  in blocks of size  $m$ . The first  $m$  outputs form the first block, the second  $m$  outputs form the second block etc. We define the vector sequence  $\{\underline{y}_k\}$  as

$$\begin{aligned}\underline{y}_0 &= (y_0, \dots, y_{m-1}) \\ \underline{y}_1 &= (y_m, \dots, y_{2m-1}) \\ \\ \underline{y}_k &= (y_{km}, \dots, y_{(k+1)m-1})\end{aligned}$$

and consider the following sub-optimum metric

$$\Gamma_{\text{sub}}(x^{lm}, y^{lm}) \triangleq \log_2 \frac{P(\underline{y}^l | \underline{x}^l)}{\prod_i w(\underline{y}_i)} - lmR \quad (2.7)$$

Note that this metric differs from the optimum metric of equation 1.12 in that it assumes that consequent  $m$  tuples of the output sequence are independent and identically distributed.  $\Gamma_{\text{sub}}(x^{lm}, y^{lm})$  may be computed easily since the output p.d.f. is specified by only  $m$  arguments.

In our simulations we make Gaussian approximation to the sequence  $\{\underline{y}_k\}$ . The results of simulations with  $\Gamma_{\text{sub}}$  and  $m = 1$  are presented in Section 2.2.3 and Appendix A. Simulations yield that this metric can not achieve the cutoff rate, as will be addressed in Section 2.2.3 .

One can use the same metric with larger values of  $m$ , taking into account the correlations among  $m$  consecutive symbols. The performance is expected to be no worse than that for  $m=1$  since  $\Gamma_{\text{sub}} = \Gamma$  as  $m \rightarrow \infty$ . The number of metric computations per decoded bit,  $\tilde{C}_M$ , for  $m = 1$  and  $m = 10$  are given in Figure 2.3 for a channel whose symmetric cutoff rate is 0.9930. Simulations yield that  $\tilde{C}_M$  decreases monotonically with increasing  $m$ . Therefore one may approach the cutoff rate by increasing  $m$  at the expense of increasing the complexity of the metric.

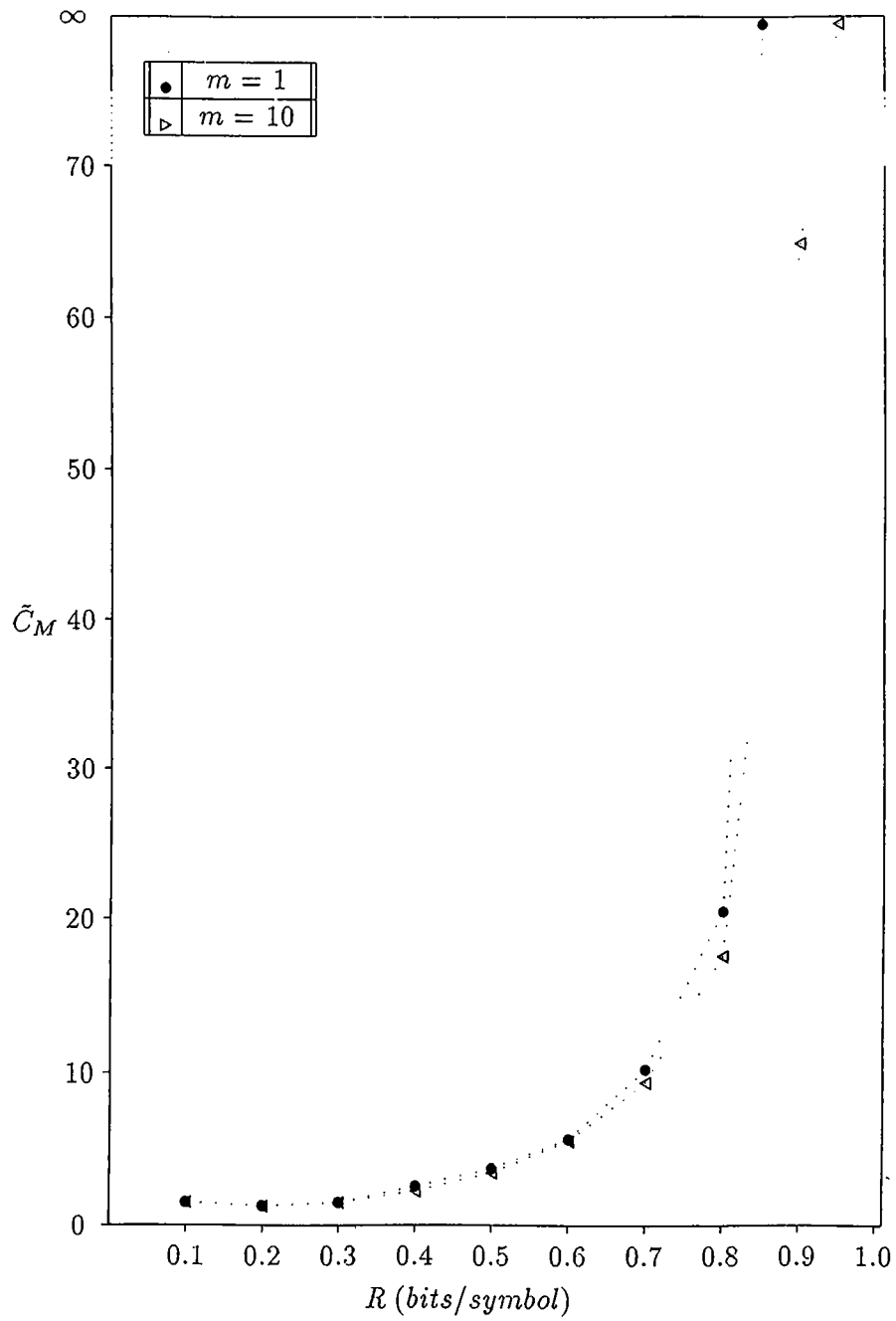


Figure 2.3. Computation of sequential decoder for different metrics.

### 2.2.3 Simulation Results

The average number of computations that a sequential decoder makes diverges as the code rate approaches the cutoff rate. This fact enables us determine upper and lower bounds to the cutoff rate through simulations. In our simulations we trace the rate span with steps of size 0.1 and label the largest rate for which the average number of computations is finite as a lower bound to the cutoff rate.

Figure 2.4 shows the number of metric computations per decoded bit,  $\tilde{C}_M$ , as a function of code rate <sup>2</sup>. Lower bounds to the cutoff rates for different values of  $T_c$  are given in Figure 2.5. Note that since the decoding metric is not optimum, there are cases that the lower bound that is obtained through simulations is less than  $\tilde{R}_0^b - 0.1$ .

Lower bounds to  $S_0$  as a function of  $T_c$ , the primary point of interest to us, are given in Figure 2.6. These quantities are obtained from the data of Figure 2.5 by Equation 2.4, therefore the theoretical and practical results inherently differ. Observe that both theoretical and simulation results indicate that it is possible to make use of sequential decoding at information densities larger than 2.0.

Note that these plots show that the cutoff rate can be equal to 1.0 for nonzero noise power. Consider the channel filter in Figure 2.2 as a part of the channel encoder. Then the remaining part of the picture is an AWGN channel with unquantized outputs, because the channel filter is a convolutional encoder in the real field. We intuitively expect that there is a nonzero noise power for which the cutoff rate of the encoding scheme exceeds 1.0. Since the channel filter is a rate 1.0 encoder, the average number of computations converge when the trellis encoder is operating at rate 1.0 as is the case for  $T_c \in [12.40\eta\text{sec}, 14.35\eta\text{sec}]$ . Hence we conjecture that for every ISI pattern there is a nonzero noise power such that uncoded transmission can be achieved with a sequential decoder with high probability, and the error probability is determined by the ISI length.

As a final note, Figure 2.4 indicates that even below the cutoff rate one may have to make considerable amount of computation, so one may be interested in the maximum information density that can be achieved by limiting the number of computations per decoded bit. In Appendix A we present the average computation results for rates  $\frac{1}{5}, \frac{2}{5}, \frac{3}{5}, \frac{4}{5}, \frac{1}{2}$  and  $\frac{1}{1}$ . As expected, we observe that the computation of the decoder increases with the denominator of the rate.

---

<sup>2</sup>To see the behavior of computation clearly, all code rates are implemented by mapping  $s$  source symbols into 10 channel symbols, for example the rate 0.2 is rate  $\frac{2}{10}$  rather than  $\frac{1}{5}$ .

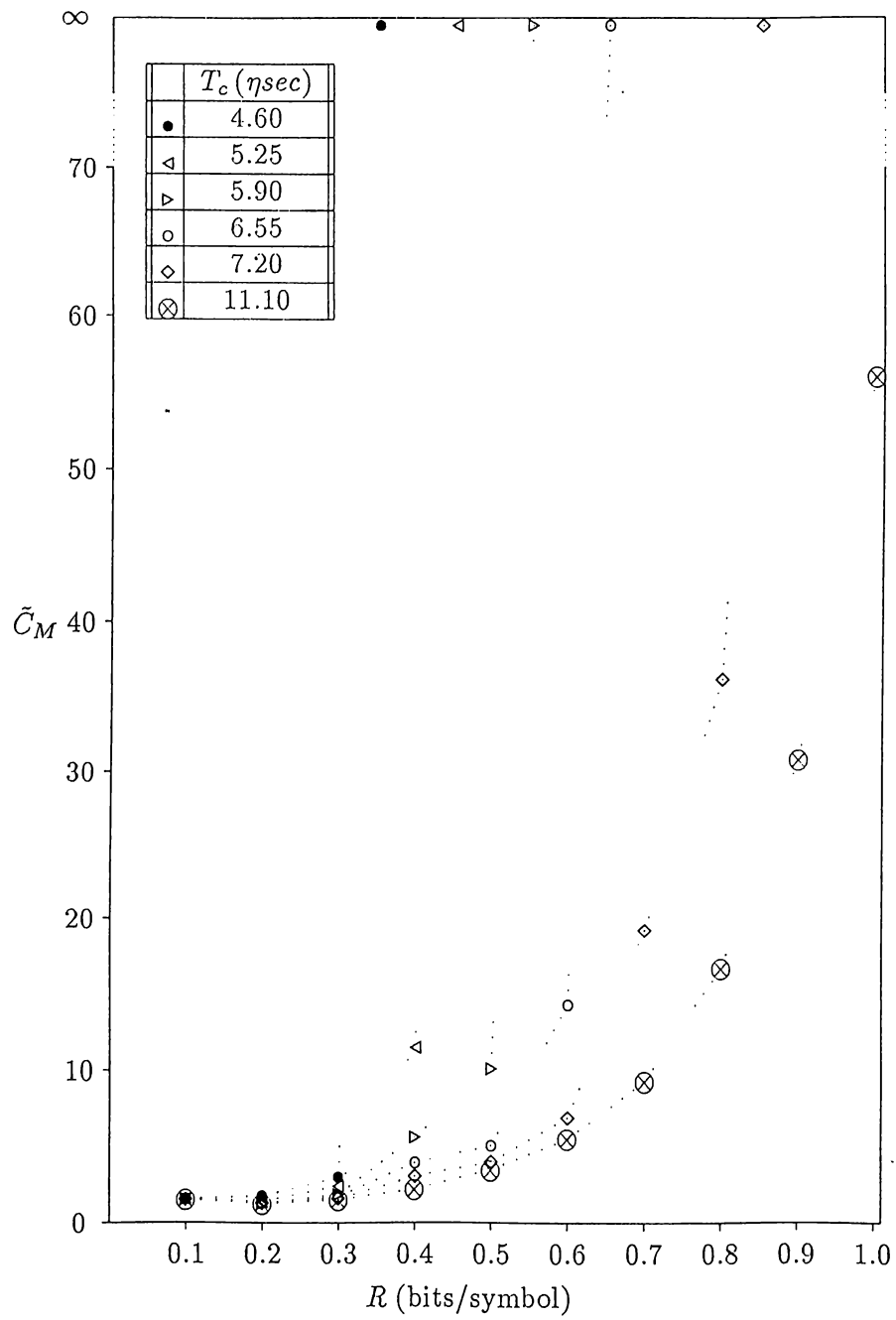


Figure 2.4. Computation of sequential decoder for different values of  $T_c$ .

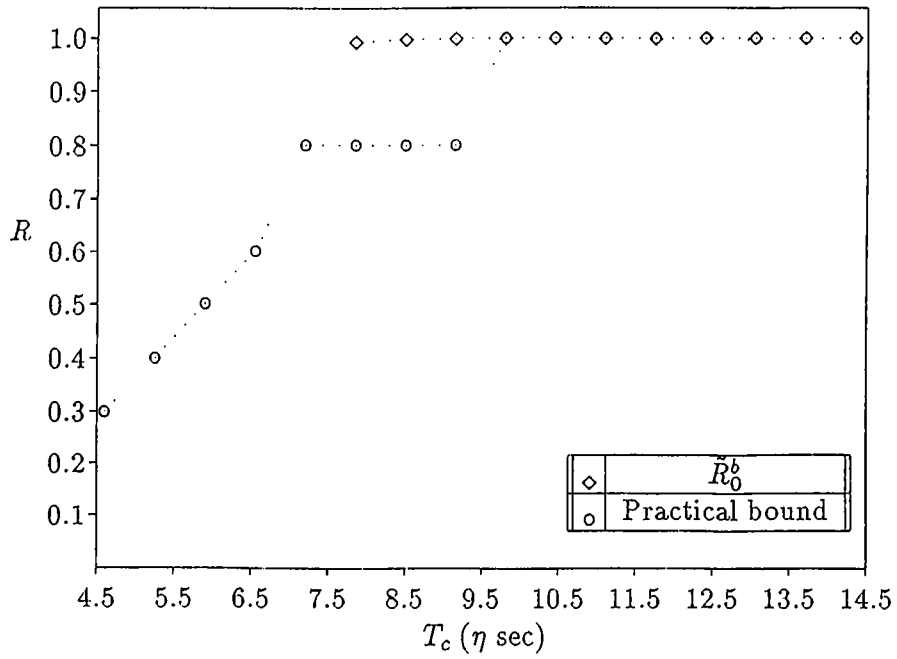


Figure 2.5. Lower bounds to the cutoff rate of the intersymbol interference channel through simulations, and the symmetric cutoff rate.



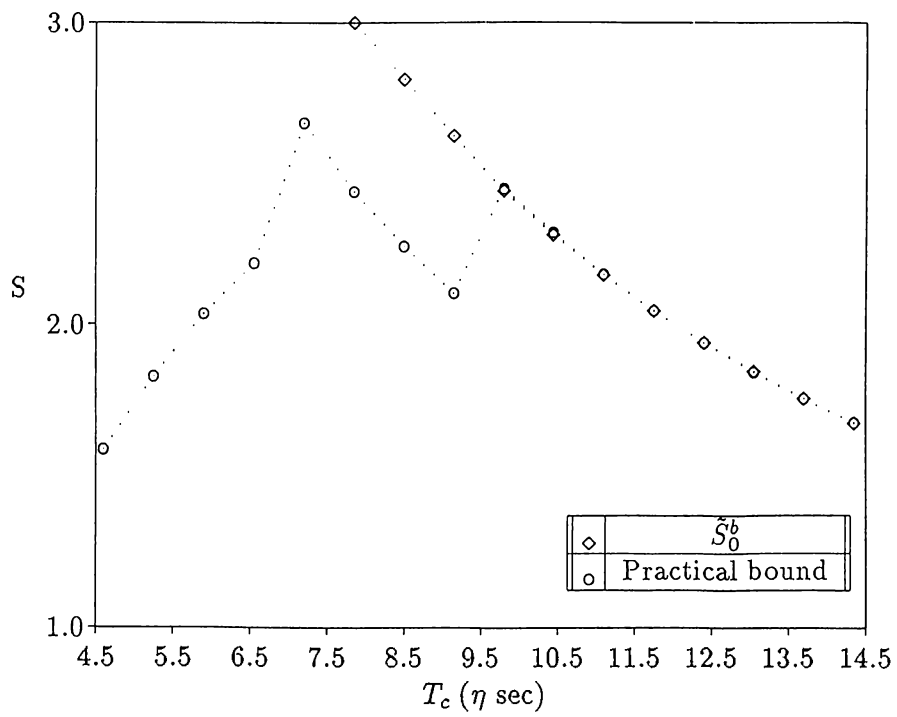


Figure 2.6. Lower bounds to the maximum information densities where sequential decoding can be used.

## Chapter 3

# CONCLUSION

In this thesis work, we studied sequential decoding algorithms on intersymbol interference channels. In particular we considered the noisy magnetic recording channel, and compared the performance of trellis coding along with sequential decoding with some previous results on the basis of noise immunity. We observed that one can achieve arbitrary positive coding gains at information densities of practical interest, where coding schemes examined by Immink [9] show coding loss.

The basic problem with sequential decoding on channels with memory is the decoding metric selection. The known optimum metrics prove impractical, hence one has to seek sub-optimum metrics which can be computed in practice. In this study we introduced such a metric which is equivalent to the optimum one in a limiting sense. Simulations yield that this metric can not achieve the cutoff rate in general, but still it is adequate for achieving coding gains at relevant information densities.

## Appendix A

# COMPUTATION RESULTS OF SEQUENTIAL DECODING

In this thesis work, the simulations were performed by encoding 2000 i.i.d. source bits. The channel filter coefficients  $\{f_k\}$  were derived from the autocorrelation coefficients  $\{R_k\}$  by using signal reconstruction from magnitude techniques.

The  $D$  transform of a sequence  $\{x_k\}$  is defined as

$$x(D) = x_0 + x_1D + x_2D^2 + \dots \quad (\text{A.1})$$

Then, Equation 1.7 indicates that [1]

$$R(D) = f(D)f(D^{-1}) \quad (\text{A.2})$$

when  $D = e^{-j\frac{2\pi}{(2L+1)}w}$  we have

$$|f(w)|^2 = R(w) \quad (\text{A.3})$$

where  $f(w)$  and  $R(w)$  are the  $(2L + 1)$  point Discrete Fourier Transforms of the signals  $\{f_k\}$  and  $\{R_k\}$  respectively. Since we know that only the first  $L + 1$  elements of  $\{f_k\}$  can be nonzero and the magnitude of  $f(w)$ , we use projections onto convex sets technique to find  $\{f_k\}$ . Note that the set described by Equation A.3 is not convex, hence the iterations are not guaranteed to converge to a solution. However for all the values of  $T_c$  in which we were interested in this study, this technique produced valid solutions.

ISI becomes more severe with decreasing  $T_c$ , so every  $T_c$  value induces a different discrete channel and cutoff rate. In the simulations, for a certain value of  $T_c$ , we trace the rate span with step size of 0.1 by changing  $T$ . The maximum rate for which the computation of the sequential decoder converges is recorded as a lower bound to the cutoff rate for that value of  $T_c$ .

Since it is highly probable that any selected code will not be far from optimum, the codes were chosen at random, and throughout the simulations the constraint length was 30. The average number of errors was 0 in all cases for which the computation of the sequential decoder was finite.

In the following we tabulate the average computation results of the sequential decoder. These involve the number of metric computations per decoded bit,  $\tilde{C}_M$ , and the number of forward hypotheses,  $\tilde{C}_F$ , per code tree node for different implementation of code rates.

$T_c(\eta\text{sec})$	Rate (bits)	$\tilde{C}_M$	$\tilde{C}_F$
4.60	1/10	1.543	1.007
	1/5	1.833	1.150
	2/10	1.759	1.233
	3/10	3.001	1.545
	2/5	$\infty$	$\infty$
	4/10	$\infty$	$\infty$
	1/2	-	-
	5/10	-	-
	3/5	-	-
	6/10	-	-
	7/10	-	-
	4/5	-	-
	8/10	-	-
	9/10	-	-
10/10	-	-	

$T_c(\eta\text{sec})$	Rate (bits)	$\tilde{C}_M$	$\tilde{C}_F$
5.25	1/10	1.531	1.001
	1/5	1.671	1.070
	2/10	1.415	1.064
	3/10	2.438	1.338
	2/5	14.441	7.487
	4/10	11.479	3.284
	1/2	$\infty$	$\infty$
	5/10	$\infty$	$\infty$
	3/5	-	-
	6/10	-	-
	7/10	-	-
	4/5	-	-
	8/10	-	-
	9/10	-	-
10/10	-	-	

$T_c(\eta\text{sec})$	Rate (bits)	$\tilde{C}_M$	$\tilde{C}_F$
5.90	1/10	1.528	1.000
	1/5	1.582	1.026
	2/10	1.299	1.006
	3/10	1.877	1.130
	2/5	3.985	2.331
	4/10	5.631	1.842
	1/2	2.340	1.401
	5/10	8.087	1.730
	3/5	$\infty$	$\infty$
	6/10	$\infty$	$\infty$
	7/10	-	-
	4/5	-	-
	8/10	-	-
	9/10	-	-
10/10	-	-	

$T_c(\eta\text{sec})$	Rate (bits)	$\tilde{C}_M$	$\tilde{C}_F$
6.55	1/10	1.528	1.000
	1/5	1.557	1.014
	2/10	1.285	1.000
	3/10	1.725	1.073
	2/5	3.055	1.872
	4/10	3.935	1.424
	1/2	1.755	1.113
	5/10	5.028	1.244
	3/5	3.750	1.823
	6/10	12.229	1.807
	7/10	$\infty$	$\infty$
	4/5	$\infty$	$\infty$
	8/10	-	-
	9/10	-	-
10/10	-	-	

$T_c(\eta\text{sec})$	Rate (bits)	$\tilde{C}_M$	$\tilde{C}_F$
7.20	1/10	1.528	1.000
	1/5	1.544	1.007
	2/10	1.285	1.000
	3/10	1.581	1.020
	2/5	2.105	1.404
	4/10	3.039	1.203
	1/2	1.705	1.088
	5/10	3.956	1.079
	3/5	2.398	1.323
	6/10	6.901	1.130
	7/10	19.212	1.534
	4/5	4.663	1.088
	8/10	36.124	1.600
	9/10	$\infty$	$\infty$
	1/1	-	-
10/10	-	-	

$T_c(\eta\text{sec})$	Rate (bits)	$\tilde{C}_M$	$\tilde{C}_F$
7.85	1/10	1.528	1.000
	1/5	1.537	1.004
	2/10	1.285	1.000
	3/10	1.537	1.004
	2/5	1.567	1.139
	4/10	2.567	1.086
	1/2	1.642	1.057
	5/10	3.716	1.041
	3/5	2.089	1.208
	6/10	5.685	1.017
	7/10	10.188	1.048
	4/5	4.151	1.477
	8/10	20.508	1.118
	9/10	$\infty$	$\infty$
	1/1	-	-
10/10	-	-	

$T_c(\eta\text{sec})$	Rate (bits)	$\tilde{C}_M$	$\tilde{C}_F$
8.50	1/10	1.528	1.000
	1/5	1.535	1.003
	2/10	1.285	1.000
	3/10	1.525	1.000
	2/5	1.361	1.037
	4/10	2.335	1.029
	1/2	1.584	1.027
	5/10	3.588	1.022
	3/5	1.609	1.031
	6/10	5.493	1.000
	7/10	9.356	1.003
	4/5	2.335	1.029
	8/10	18.076	1.043
	9/10	$\infty$	$\infty$
	1/1	-	-
10/10	-	-	

$T_c(\eta\text{sec})$	Rate (bits)	$\tilde{C}_M$	$\tilde{C}_F$
9.15	1/10	1.528	1.000
	1/5	1.534	1.002
	2/10	1.285	1.000
	3/10	1.525	1.000
	2/5	1.307	1.010
	4/10	2.255	1.009
	1/2	1.615	1.043
	5/10	3.508	1.009
	3/5	1.561	1.013
	6/10	5.493	1.000
	7/10	9.356	1.003
	4/5	2.271	1.013
	8/10	16.668	1.000
	9/10	$\infty$	$\infty$
	1/1	-	-
10/10	-	-	



$T_c(\eta\text{sec})$	Rate (bits)	$\tilde{C}_M$	$\tilde{C}_F$
9.80	1/10	1.528	1.000
	1/5	1.533	1.002
	2/10	1.285	1.000
	3/10	1.525	1.000
	2/5	1.301	1.007
	4/10	2.223	1.001
	1/2	1.601	1.035
	5/10	3.476	1.004
	3/5	1.553	1.010
	6/10	5.493	1.000
	7/10	9.356	1.003
	4/5	2.255	1.009
	8/10	16.668	1.000
	9/10	31.209	1.008
	1/1	15.029	7.655
10/10	56.523	1.004	

$T_c(\eta\text{sec})$	Rate (bits)	$\tilde{C}_M$	$\tilde{C}_F$
10.45	1/10	1.528	1.000
	1/5	1.532	1.001
	2/10	1.285	1.000
	3/10	1.525	1.000
	2/5	1.293	1.003
	4/10	2.215	1.000
	1/2	1.586	1.029
	5/10	3.460	1.002
	3/5	1.537	1.004
	6/10	5.493	1.000
	7/10	9.292	1.000
	4/5	2.239	1.005
	8/10	16.668	1.000
	9/10	30.780	1.000
	1/1	16.067	8.168
10/10	56.011	1.000	

$T_c(\eta\text{sec})$	Rate (bits)	$\tilde{C}_M$	$\tilde{C}_F$
11.10	1/10	1.528	1.000
	1/5	1.532	1.001
	2/10	1.285	1.000
	3/10	1.525	1.000
	2/5	1.291	1.002
	4/10	2.215	1.000
	1/2	1.584	1.027
	5/10	3.444	1.000
	3/5	1.537	1.004
	6/10	5.493	1.000
	7/10	9.292	1.000
	4/5	2.231	1.003
	8/10	16.668	1.000
	9/10	30.780	1.000
	1/1	16.957	8.808
10/10	56.011	1.000	

$T_c(\eta\text{sec})$	Rate (bits)	$\tilde{C}_M$	$\tilde{C}_F$
11.75	1/10	1.528	1.000
	1/5	1.530	1.001
	2/10	1.285	1.000
	3/10	1.525	1.000
	2/5	1.291	1.002
	4/10	2.215	1.000
	1/2	1.582	1.027
	5/10	3.444	1.000
	3/5	1.533	1.002
	6/10	5.493	1.000
	7/10	9.292	1.000
	4/5	2.231	1.003
	8/10	16.668	1.000
	9/10	30.780	1.000
	1/1	17.838	9.040
10/10	56.011	1.000	

$T_c(\eta\text{sec})$	Rate (bits)	$\bar{C}_M$	$\bar{C}_F$
12.40	1/10	1.528	1.000
	1/5	1.530	1.001
	2/10	1.285	1.000
	3/10	1.525	1.000
	2/5	1.291	1.002
	4/10	2.215	1.000
	1/2	1.584	1.027
	5/10	3.444	1.000
	3/5	1.533	1.002
	6/10	5.493	1.000
	7/10	9.292	1.000
	4/5	2.231	1.003
	8/10	16.668	1.000
	9/10	30.780	1.000
	1/1	18.648	9.440
10/10	56.011	1.000	

$T_c(\eta\text{sec})$	Rate (bits)	$\bar{C}_M$	$\bar{C}_F$
13.05	1/10	1.528	1.000
	1/5	1.530	1.001
	2/10	1.285	1.000
	3/10	1.525	1.000
	2/5	1.289	1.001
	4/10	2.215	1.000
	1/2	1.568	1.019
	5/10	3.444	1.000
	3/5	1.533	1.002
	6/10	5.493	1.000
	7/10	9.292	1.000
	4/5	2.231	1.003
	8/10	16.668	1.000
	9/10	30.780	1.000
	1/1	19.390	9.805
10/10	56.011	1.000	

$T_c(\eta\text{sec})$	Rate (bits)	$\bar{C}_M$	$\bar{C}_F$
13.70	1/10	1.528	1.000
	1/5	1.530	1.001
	2/10	1.285	1.000
	3/10	1.525	1.000
	2/5	1.287	1.001
	4/10	2.215	1.000
	1/2	1.584	1.027
	5/10	3.444	1.000
	3/5	1.529	1.001
	6/10	5.493	1.000
	7/10	9.292	1.000
	4/5	2.223	1.001
	8/10	16.668	1.000
	9/10	30.780	1.000
	1/1	16.197	8.099
10/10	56.011	1.000	

$T_c(\eta\text{sec})$	Rate (bits)	$\bar{C}_M$	$\bar{C}_F$
14.35	1/10	1.528	1.000
	1/5	1.532	1.001
	2/10	1.285	1.000
	3/10	1.525	1.000
	2/5	1.287	1.001
	4/10	2.215	1.000
	1/2	1.584	1.027
	5/10	3.444	1.000
	3/5	1.529	1.001
	6/10	5.493	1.000
	7/10	9.292	1.000
	4/5	2.223	1.001
	8/10	16.668	1.000
	9/10	30.780	1.000
	1/1	20.743	10.473
10/10	56.011	1.000	

# Bibliography

- [1] G. D. Forney, "Maximum-likelihood sequence estimation of digital sequences in the presence of intersymbol interference," *IEEE Trans. Inform. Theory*, vol. IT-18, pp. 363-378, May 1972.
- [2] W. U. Lee and F. S. Hill, "A maximum likelihood estimator with decision-feedback equalization," *IEEE Trans. Commun.*, vol. COM-25, pp. 971-980, Sept. 1977.
- [3] M. V. Eyüboğlu and S. U. H. Qureshi, "Reduced state sequence estimation for coded modulation on intersymbol interference channels," *IEEE J. Select. Areas Commun.*, vol. 7, pp. 989-995, Aug. 1989.
- [4] A. Duel-Hallen and C. Heegard, "Delayed decision feedback estimation," *IEEE Trans. Commun.*, vol. COM-37, pp. 428-436, May 1989.
- [5] J. W. M. Bergmans, S. A. Rajput and F. A. M. Van De Laar, "On the use of decision feedback for simplifying the viterbi detector," *Philips J. Res.* vol. 42, pp. 399-428, 1987.
- [6] N. Seshadri and J. B. Anderson, "Decoding of severely filtered modulation codes using the (m,l) algorithm," *IEEE J. Select. Areas Commun.*, vol. 7, pp. 1006-1016, Aug. 1989.
- [7] R. W. Chang and J. C. Hancock, "On receiver structures for channels having memory," *IEEE Trans. Inform. Theory*, vol. IT-12, pp.463-468, Oct. 1966.
- [8] K. Abend and B. D. Fritchman, "Statistical detection for communication channels with intersymbol interference," *Proc. IEEE*, vol. 58, pp. 779-785, May 1970.
- [9] K. A. S. Immink, "Coding techniques for the noisy magnetic recording channel: a state-of-the-art report," *IEEE Trans. Commun.*, vol. COM-37, pp. 413-419, May 1989.
- [10] R. G. Gallager, *Information Theory and Reliable Communication*. New York, NY: Wiley, 1968.
- [11] L. N. Lee, "On optimal soft-decision modulation," *IEEE Trans. Inform. Theory*, vol. IT-22, pp. 437-444, July 1976.

- [12] W. Hirt, "New applications and properties of the symmetric cutoff rate of channels with intersymbol interference," *Proc. ISIT '88*, Kobe, Japan, June 1988.
- [13] G. D. Forney, "Lower bounds on error probability in the presence of large intersymbol interference," *IEEE Trans. Commun.*, vol. COM-20, pp. 76-77, Feb. 1972.
- [14] J. K. Wolf and G. Ungerboeck, "Trellis coding for partial partial-response channels," *IEEE Trans. Commun.*, vol. COM-34, pp. 765-773, Aug. 1986.
- [15] E. Arıkan, "Sequential decoding on multiple access channels," *IEEE Trans. Inform. Theory*, vol. IT-34, pp. 246-259, March 1988.